

Article

Using Remote Sensing to Quantify Vegetation Change and Ecological Resilience in a Semi-Arid System

Xia Cui ¹, Cerian Gibbes ^{2*}, Jane Southworth ³ and Peter Waylen ³

¹ The State Key Laboratory of Grassland Farming Systems, College of Pastoral Agriculture Science and Technology, Lanzhou University, Lanzhou 730020, China; E-Mail: xiacui2006@163.com

² Department of Geography and Environmental Studies, University of Colorado, Colorado Springs, 1420 Austin Bluffs Parkway, Colorado Springs, CO 80918, USA

³ Department of Geography & Land Use and Environmental Change Institute (LUECI), University of Florida; 3141 Turlington Hall, P.O. Box 117315, Gainesville, FL 32611, USA; E-Mails: jsouthwo@ufl.edu (J.S.); prwaylen@ufl.edu (P.W.)

* Author to whom correspondence should be addressed; E-Mail: cgibbes@uccs.edu; Tel.: +1-719-255-3534; Fax: +1-719-255-4066.

Received: 15 February 2013; in revised form: 13 March 2013 / Accepted: 18 March 2013 /

Published: 8 April 2013

Abstract: This research extends upon land cover change studies by incorporating methodological approaches, which are compatible with heterogeneous ecosystems, are able to link landscape changes to system processes, such as climate change, and provide potential linkages to concepts of ecological resilience. The study region in southern Africa experienced a significant climatic shift in the 1970s, resulting in drier conditions. The state of these ecosystems and their response to such climatic shock is quantified in terms of vegetation amount and heterogeneity. We monitor these characteristics pre- and post-disturbance using a Landsat image series and examine the utility of continuous characterizations of land cover for measuring ecosystem resilience. Land cover change is evaluated using a mean-variance analysis in concert with a spatial persistence analysis. This investigation indicates that although the impact of the decreased precipitation is evident in the 1980s, recovery occurred by the 1990s and 2000s. We found the continuous methodological approach used holds potential for studying heterogeneous landscapes within a resilience framework.

Keywords: savanna; vegetation cover; NDVI; climate change; resilience; land cover; Landsat

1. Introduction

Savanna landscapes occupy the continuum between forest and grasslands, consisting of a continuous layer of grasses interrupted by trees and shrubs [1]. These landscapes, with varying proportions of grasses, trees and shrubs, exist within regions of highly variable rainfall, a climatic characteristic that limits the development of a closed canopy [2]. The inherent heterogeneity of savannas is partially maintained by complex interactions amongst biophysical and human caused drivers of change. While water availability and soil nutrients are the primary determinants of savanna composition [2], they are coupled with the local factors of fire, herbivory and anthropogenic land use to create and maintain spatial heterogeneity within savanna landscapes [3,4]. Human and herbivore-related impacts on landscape change are particularly influential at finer scales. Changes in savanna composition are occurring globally as a result of variations in the interactions of these local drivers of landscape change and changes in climate.

With global climate change predictions indicating that these regions will experience increased frequency and intensity of extreme events (in particular, droughts), there is a high likelihood of drastic vegetation change potentially accompanied by decreases in biodiversity. Such changes would lead to modifications in resource availability for populations living within semi-arid savannas. Therefore, concerns about land change and degradation are inherently intertwined with concerns about human well-being and poverty. The socio-ecological implications of possible degradation in semi-arid regions necessitate an improved understanding of the ecological resilience of these regions [5].

The use of land cover change analyses based on classification schemes provides useful depictions of the landscape for management purposes, highlights land cover conversions and provides data on the basic spatial and temporal distribution of discrete land cover classes ideal for modeling purposes. Additionally, land cover classifications offer a standardized approach for measuring environmental parameters and monitoring the state of ecosystems [6]. However, in highly heterogeneous ecosystems, such as savannas, land cover classifications have moderate accuracy and can be inconsistent (both spatially and quantitatively) with field observations and global land cover maps [6–8]. Furthermore, the reliance on land cover classifications has led to more emphasis on studies that examine land cover conversions rather than modifications [9]. This emphasis is accompanied by a focus on post-impact or shift landscapes, rather than highlighting approaching thresholds [10], which are often of more concern when employing land cover analyses to examine changes in ecosystem state. As such, evaluations of methodologies, which help highlight these thresholds of change or likely pathways of modifications, are essential to the progression of land change science.

Southern African Savannas and Resilience

Climate change is expected to exert significant influence on savanna vegetation, as spatial and temporal patterns of precipitation are strongly correlated with vegetation composition [11–15]. Changes in global ocean-atmosphere interactions and resultant precipitation patterns have been observed in the mid- to late 1970s [16,17], potentially initiated by differences in circulation in the North Pacific [18]. Over the savanna regions of southern Africa, this shift has been associated with increasing air temperatures and prolonged dry periods [17,19,20], often in association with warm phases of El

Niño/Southern Oscillation (ENSO). This increased connectivity with the major cause of global climate variability is postulated to be the result of the increased influence of the ENSO phenomenon on the Indian Ocean [21,22], a principal source of moisture to the study area [23]. Partially driven by climate, southern African savannas are thought to be currently experiencing dry land degradation, recurrently associated with changes in floral and faunal biodiversity [24,25]. Such degradation can be quantified in terms of vegetation attributes, including (though not limited to) plant cover, heterogeneity and productivity [26,27]. Degradation in the southern African context is defined by a loss of the variation in vegetation and unidirectional shifts in vegetation composition towards shrub dominated landscapes [28,29].

Long-term monitoring of southern African savannas is needed to enhance the understanding of broad-scale changes in vegetation and the possible relationship between such changes and ecosystem resilience. Ecosystem resilience, defined as the capacity of a system to absorb disturbances and maintain essential structures, processes and feedbacks [30], can be difficult to quantify, because it is a condition relative to an earlier state [31]. However, examining ecosystem characteristics, which serve as indicators of degradation across large spatial and temporal scales, is one way by which the effect of disturbances on landscapes may be considered. Ecosystem indicators, such as vegetation status, can be analyzed using spatially aggregate and/or spatially explicit methods to measure resilience [27]. Westman and O’Leary [32] identify four ways in which an indicator can be measured with regard to ecological resilience: elasticity, amplitude, malleability and damping (Table 1). Each of these measures the state of the indicator (*i.e.*, vegetation) in comparison to a reference state and considers the capacity of the system to absorb disturbances, while retaining structure and function. The expression of each measure is dependent upon the ecosystem characteristic being observed and, thus, differs by characteristic, but allows for comparison of any one of them across space and time [32]. Westman and O’Leary [32] rely largely on field data and a simulation model; however, similar approaches have been implemented utilizing remotely sensed vegetation data [27,33].

Table 1. Indicator measures of system resilience, identified by Westman and O’Leary [32], modified from Washington-Allen *et al.* [27].

Indicator Measure	Definition
Elasticity	The period of restoration to a reference condition following a disturbance
Amplitude	Magnitude of change resulting from a disturbance
Malleability	Degree to which the state established after a disturbance differs from the original state
Damping	Pattern of oscillation in a system following disturbance

The quantity and heterogeneity of vegetation within African savannas are ecosystem characteristics that reflect the state of the system and can be quantified over large spatial and temporal extents using remote sensing. The quantity of biomass provides a useful indicator of the contribution of vegetation to ecosystem resilience and, correspondingly, its ability to modify other landscape shaping parameters, such as fire [34,35]. Vegetation presence and diversity directly relates to factors impacting ecological functioning, such as herbivory, surface temperatures and soil moisture content [36]. Vegetation indices offer ideal measures of amounts of vegetation and variations in vegetation distribution, both over space and time. The established relationship between vegetation indices and biomass forms the basis of land

cover analyses, which rely on vegetation indices to provide a continuous representation of land cover. The normalized difference vegetation index (NDVI) is particularly useful for measuring amounts of photosynthesizing biomass in semi-arid and savanna regions [37], where it does not saturate [13]. While there are potential limitations to the use of NDVI in this region, due to soil type and exposure [38], the time-frame for this study, 1975 onwards, and the multiple platforms used (Landsat Multispectral Scanner (MSS) and Landsat Thematic Mapper (TM)) from which NDVI may be obtained at a fine spatial scale as necessary for this analysis, make the index an ideal starting point, which is comparable to previous regional research [13,39,40].

This study utilizes remotely sensed data and a framework proposed by Westman and O'Leary [32] and employed by Washington-Allen *et al.* [27] to examine the value of using continuous measures of land cover within a resilience framework for studying southern African savannas. The state of the vegetation as measured through a vegetation index is determined in order to explore temporal and spatial changes in the distribution of vegetation, following the disturbance to the system resulting from the climate shift in the mid- to late 1970s [16,20]. The response of vegetation is examined with reference to the state of the pre-disturbance landscape. First, mean annual precipitation from 1950 to 2008 are analyzed to identify the effect of the global climate shift on local precipitation patterns. The following questions are then asked: (1) is this approach useful to study landscape changes over a greater temporal extent while still maintaining high spatial fidelity; (2) can this framework help link the biological and climatological systems in such a way that we can begin to understand or hypothesize regarding the system resilience? In addition to these more methodological questions, we are also interested in the actual changes being studied here and their implications for this region; as such we ask: (3) what are the long-term vegetation trends post disturbance; (4) does the system return to a similar state with regard to vegetation amount and variance; and (5) how does the vegetation trend vary spatially?

2. Materials and Methods

2.1. Study Area

The study area (~80,728 km²) is located in southern Africa, including portions of Angola, Zambia, Botswana and Namibia (Figure 1). The study area encompasses much of the proposed Kavango-Zambezi Transboundary Conservation Area (KAZA), which aims to link wildlife conservation and development efforts across the four countries and Zimbabwe and, as such, is of significant ecological and social importance to southern Africa [41]. Community and national economies are heavily dependent upon wildlife tourism, and therefore, changes in vegetation, which may directly impact wildlife species distributions, are not only of ecological concern, but also of economic import. The relatively low human population density throughout the study area and the limited use of exclusionary conservation practices enabling wildlife movement results in land cover changes being predominantly driven by broader physical phenomenon, such as climate, particularly at the landscape scale. Fire is an important land cover modifier in this region, though with the exception of anomalously large extent fires and the low human population in the study area, this further focuses the analysis presented below on the role of climate as the principal driver of landscape scale vegetation patterns. This region straddles the downstream portions of 3 major regional water courses, the

Okavango, Kwando and Zambezi Rivers. Until the late 1970s, these basins were linked seasonally by eastward flowing water; however, since the mid- to late 1970s, the basins have remained unconnected, with the waters of the Okavango and Kwando flowing into closed basins. The climate is tropical savanna with three seasons: a hot dry season (August–October), a hot wet season (November–April) and a cool dry season (May–July). Annual precipitation ranges from under 400 mm to just over 1,300 mm/yr and is characterized by high temporal interannual variability of precipitation, with totals increasing and the coefficient of variability decreasing towards the northern portion of the study area [42]. Soils are primarily Kalahari sand, which is nutrient-poor. The vegetation is dominated by a variety of annual and perennial grasses, dominant woodlands (ex. *Colophospermum mopane* woodlands), mixed woodlands and mixed shrub lands.

Figure 1. Study area situated within the proposed Kavango-Zambezi Transboundary Conservation Area (KAZA).



2.2. Data Collection and Analysis

2.2.1. Precipitation Data

Station data from Maun, Botswana, for 1950–2008 are examined in terms of their precipitation patterns pre- and post- the documented global climate shift of the 1970s. The Maun station possesses one of the few long-term, reliable precipitation records within the study area. The data are sub-divided into two time periods—1950–1970 and 1980–2008—leaving a nine year buffer surrounding the putative climate shift, thereby avoiding the possibility of an inaccurate identification of the shift or the inclusion of data from any transitional period between the two periods and regimes. Given the

considerable interannual variability of precipitation and its highly skewed nature in semi-arid regions, standard parametric tests of changes in means and variances are inappropriate. Instead, the entire historic record—1950–2008—is divided into terciles. If there are no systematic changes in rainfall properties, any sub-sample of that population (such as 1950–1970 or 1980–2008) should contain roughly equal proportions of observations from each tercile class. Under such an hypothesized random sampling scheme, the probability of observing any number of observations from one particular tercile is determined by the hypergeometric probability distribution in which N represents the total population (1950–2008 = 59), the size of the sub-sample (*i.e.*, 1950–1970, $n = 21$, or 1980–2008, $n=29$) and the number of the total population possessing the characteristic of interest (e.g., number of observations in the upper tercile or those in the lower; $k =$ approximately 19). The actual number of observations in a particular tercile during one of these two periods can then be compared to the probability of such an outcome under the null hypothesis of randomness and the null rejected or not, accordingly. Thus, in the pre-1970 period, one would expect to see approximately one third (~ 7) of the observations characterized as ‘wet years’—upper tercile—and one third (~ 7) characterized as ‘dry years’—lower tercile—and between 1980 and 2008, there should be nine of each, both with known probabilities of other numbers of observations distributed about them.

2.2.2. Image Collection and Processing

A multi-temporal and multi-spectral dataset was used for this study (Table 2). Fifteen Thematic Mapper (TM) images and seven Landsat Multispectral Scanner (MSS) images that covered the study area were acquired, all with less than 10% cloud cover, yielding a dataset that spans the time period 1973–2009. Dry season imagery was acquired to ensure limited cloud cover, for seasonal consistency and to monitor the more persistent vegetation cover of perennials and to avoid shorter-term variation from annuals and other sources of ephemeral vegetation cover (e.g., greening up following a rain event, rather than longer term variation as a result of longer temporal changes, as noted by Townshend and Justice in 1986 [15] and Archibald and Scholes in 2007 [43]). Landsat TM and MSS compatibility was ensured using direct matching of red and near-infrared bands across the two platforms [44]. All image analysis was conducted using ERDAS Imagine 9.2.

The images were georectified using a nearest neighbor resampling algorithm (root-mean-square error (RMSE) of less than 0.5 for all images) and projected to Universal Transverse Mercator (UTM) WGS 84 Zone 34 South. Image calibration was completed to correct for sensor and atmospheric variation using the CIPEC methodology [45] and Landsat MSS and TM post-launch calibration gains and biases from tables and formula provided by Markham and Barker [46]. The image footprints were mosaicked to produce a continuous dataset for each date (7 scenes for Landsat MSS and 5 scenes each for Landsat TM). The normalized difference vegetation index (NDVI) was then derived for each mosaic date, as this continuous surface is more appropriate of the highly heterogeneous landscape than a traditional classification technique. This index is used widely, allowing the findings to be interpreted easily and compared to other land cover studies across this region and to other semi-arid environments globally [35,47,48].

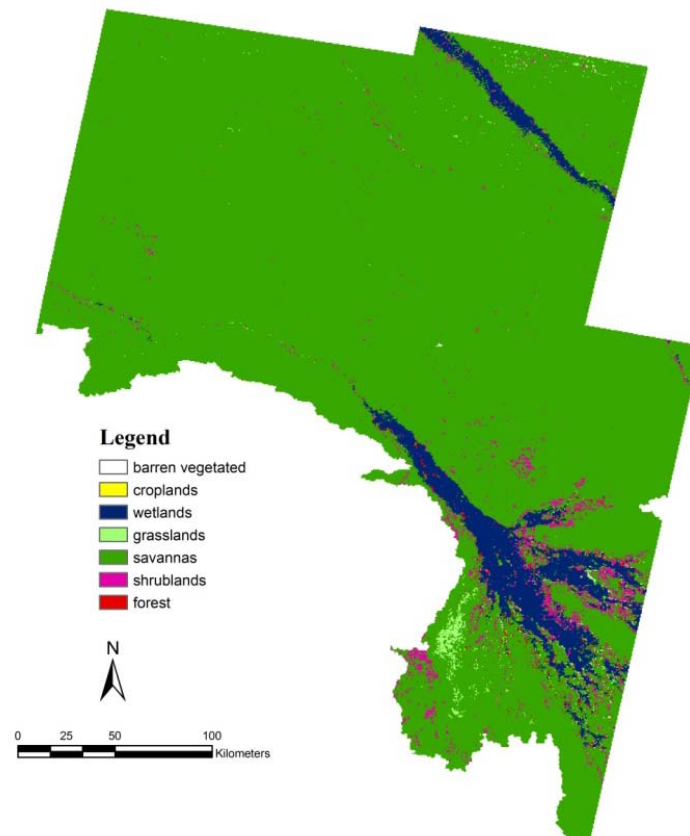
Table 2. Image characteristics of image location, date, scanner system and level of registration error for each of the image products utilized in this analysis. Root-mean-square errors (RMSEs) for the 1990 images are not included, as these images served as the reference image for registering all other images. MSS, Multispectral Scanner; TM, Thematic Mapper.

Image Footprint (path/row)	Image Date (mm-dd-yyyy)	Scanner	RMSE	Mosaic Year
187/73	06-08-1979	Landsat MSS	0.327	1970s
187/74	05-18-1976	Landsat MSS	0.497	1970s
188/72	06-30-1975	Landsat MSS	0.498	1970s
188/73	06-18-1979	Landsat MSS	0.499	1970s
188/74	06-12-1975	Landsat MSS	0.476	1970s
189/72	05-27-1973	Landsat MSS	0.496	1970s
189/73	05-27-1973	Landsat MSS	0.449	1970s
175/72	06-09-1984	Landsat TM	0.426	1984
175/72	09-05-1990	Landsat TM	---	1990
175/72	03-26-2009	Landsat TM	0.430	2009
175/73	06-09-1984	Landsat TM	0.389	1984
175/73	09-05-1990	Landsat TM	---	1990
175/73	03-26-2009	Landsat TM	0.470	2009
175/74	06-09-1984	Landsat TM	0.386	1984
175/74	27-03-1992	Landsat TM	---	1990
175/74	03-26-2009	Landsat TM	0.380	2009
176/72	07-02-1984	Landsat TM	0.362	1984
176/72	05-13-1989	Landsat TM	---	1990
176/72	05-20-2009	Landsat TM	0.452	2009
176/73	07-02-1984	Landsat TM	0.447	1984
176/73	01-04-1991	Landsat TM	---	1990
176/73	05-20-2009	Landsat TM	0.441	2009

In addition to the Landsat data, three tiles of the MCD12Q1 land cover (MODIS Terra + Aqua land cover type yearly L3 global 500 m sin grid) product of 2008 were downloaded. The land cover data was re-projected to a Universal Transverse Mercator (UTM) WGS84 projection (Zone 34 South) and clipped to the study area. The primary land cover scheme defined by the International Geosphere Biosphere Programme (IGBP) was used as a reference dataset to provide preliminary landscape categories within which vegetation trends as measured through the use of the Landsat data could be examined. The IGBP classification product is a broad classification, which is based on the canopy component philosophy presented by Running *et al.* [49]. Though limitations with this product exist, for example, over-estimation of accuracy for Africa—82.9% (Loveland *et al.* 1999)—due to, in part, the presence of the Sahara, this data product serves as an initial source for the dominant land covers present in this region, as related to a global assessment of land cover. The eleven land cover types in IGBP were merged to seven classes (barren/barely vegetated, croplands, wetlands, grasslands, savannas, shrub lands and forest) according to field survey data (Figure 2). Insufficient field observations were acquired to use for both merging of classes and testing of accuracy of the IGBP

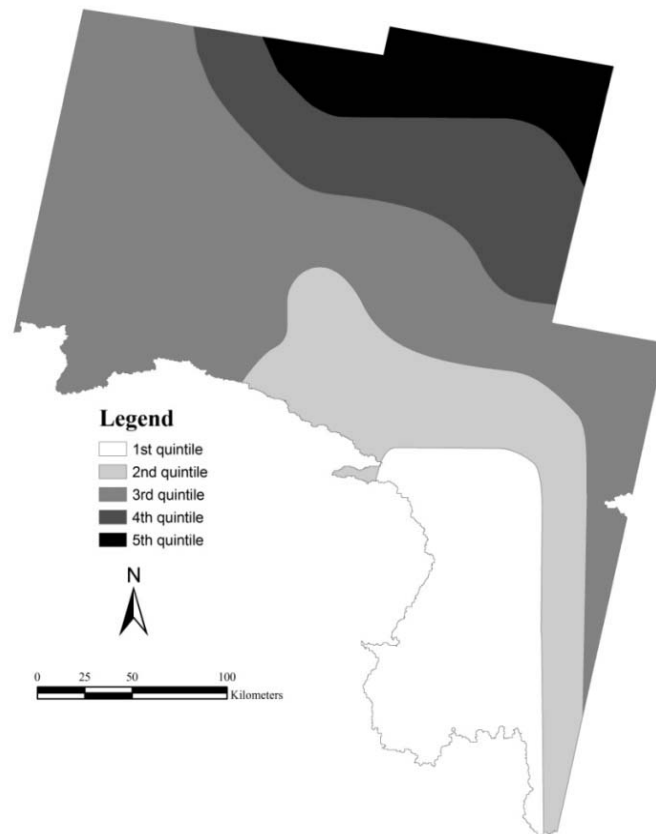
product. However, given the subjective nature of classifications in general, the difficulty of effectively employing a classification scheme in a savanna system at single or multiple scales and the prior use of this particular dataset as a reference product (e.g., Sedano *et al.* 2005 [50]), the IGBP land cover map is incorporated in the analysis to guide further examination of the change in NDVI throughout the study area.

Figure 2. Land cover classification for the study region as determined by the IGBP classification [49].



NOAA Global Precipitation Climatology Project (GPCP) version-2 monthly global gridded precipitation datum was acquired to cover the study area. This datum is a monthly analysis of surface precipitation estimated from low-orbit satellite microwave data, geosynchronous-orbit satellite infrared data and surface rain gauge observations, with a resolution of 2.5° latitude \times 2.5° longitude [51,52]. The gridded datum contained monthly rainfall values, which were summed to provide rainfall totals of water for the year. Rainfall totals (annual values) are initially employed in the analysis, as this temporal scale of variability is considered highly important for this region [5]. GPCP datasets have been widely used in climate data, and concern regarding the use of this data for Africa is largely limited to central and northern Africa [51,52]. This datum was subset into quintiles to partition the study area for separate analyses of NDVI over time, based on precipitation input to the system (Figure 3).

Figure 3. Precipitation regime classes based on precipitation quintiles calculated using the mean annual rainfall from 1972 to 2009. Actual range of data for each quintile (in order of 1–5) : 463.50mm to 523.57 mm, 538.93 mm to 582.2 mm, 575.03 mm to 582.21 mm, 605.71 to 642.93 mm, 657.04 mm to 698.57 mm.



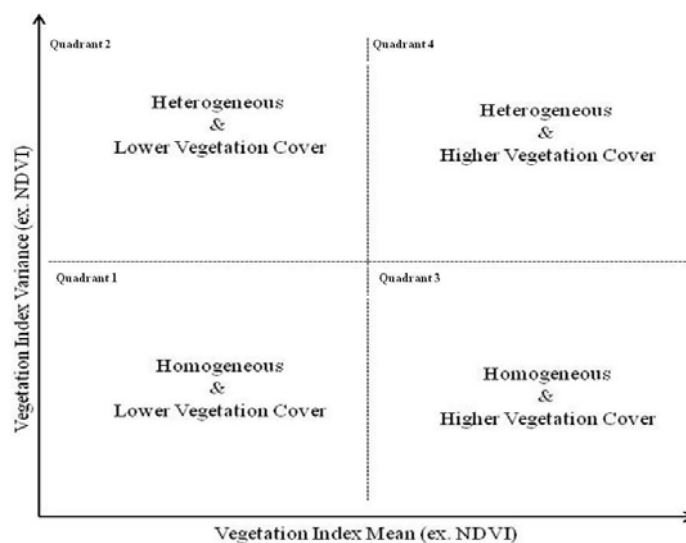
2.2.3. Mean-Variance Analysis

This research evaluates the utility remote sensing offers, in terms of the possibility to analyze changes in ecological resilience at the landscape scale using vegetation amount and heterogeneity as indicator measures. NDVI was characterized using a mean-variance analysis, which can be computed from image statistics [53] and which characterizes the temporal behavior of NDVI [27]. The approach is employed to describe the trajectory of vegetation states at set time points, across the 37-year time period, in terms of the mean NDVI, which represents the overall *amount* of vegetation within the landscape and the variance of NDVI to represent the *heterogeneity* of the vegetation cover. Considering that the Global Land Project classification scheme classifies most of this diverse region as “savanna”, essentially removing the dominant characteristic of savannas (*i.e.*, vegetation heterogeneity), experimentation with approaches, such as is used here, is needed in order to provide land cover assessments, which are suitable for analyses of extended spatial extents, yet do not remove the inherent heterogeneity of the system.

Figure 4 shows the hypothetical relationship between mean-variance and vegetation status. Each quadrant in Figure 4 offers a relative measure of heterogeneity (variance) and vegetation presence (mean). Variance is representative of the degree of landscape heterogeneity, while the mean gives an indication of vegetation quantity and is interpreted here for use in savanna systems (interpretations of

this figure are biome-specific). Quadrant 1 displays low mean and low variance values and can be considered to be representative here of degraded landscapes. Quadrant 2 exhibits low mean values, but high variance, and indicates landscapes that possibly possess a lot of bare ground and which are susceptible to disturbance. Quadrant 3 contains landscapes with high mean and low variance values, suggesting that much of the landscape has vegetation cover. Assuming the desired state for savanna at this scale consists of high vegetation cover and heterogeneity, as is suggested by [1,3,4], the high mean and high variance of quadrant 4 would be the quadrant within which observations of a healthy functioning savanna would lie. Using this framework, if a landscape moves away from Quadrant 4 to lower vegetative cover (decrease in mean NDVI) and lower heterogeneity (decrease in variance), this is a potential indicator for degradation or potential negative ecological change. If it moves towards Quadrant 4, we could argue it has recovered from a perturbation (in this instance, a decrease in precipitation), and the landscape thus demonstrates a degree of resilience at this spatio-temporal scale. The mean-variance plots for the entire landscape, individual land covers as determined by the IGBP land cover classification and the quintile classes were generated for this study.

Figure 4. Hypothetical relationship between mean-variance and vegetation status, adapted from Washington-Allen *et al.* [27].



2.2.4. Persistence Analysis

To assess NDVI change in a spatially-explicit manner, an NDVI persistence layer was calculated. The layer characterizes the direction of change in NDVI relative to the 1970s vegetation state. For each time step post-1970s (1984–1990–2009), the direction of change (*i.e.*, increase or decrease in NDVI) relative to the reference state (1970s) is determined using the following nomenclature:

$$t < t_i = +1 \quad (1)$$

$$t > t_i = -1 \quad (2)$$

$$t = t_i = 0 \quad (3)$$

where t is the initial reference state, that is, 1970s NDVI, and t_i is NDVI at each of the following time steps. By assigning the appropriate value to pixels, depending upon the direction of change, a

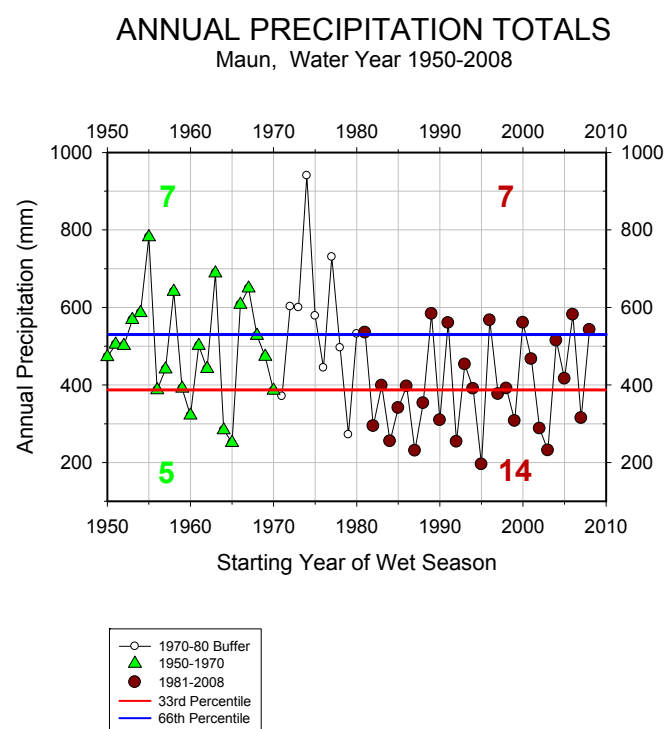
cumulative persistence layer may be calculated by summing each of the individual maps. The cumulative analysis measures direction of change over time relative to the benchmark observation of NDVI. Cumulative persistence provides a simple measure that specifies the dominant pattern of change per pixel in a spatially-explicit manner. This provides an interesting and efficient analysis, which allows for a more spatial examination of the trends under study.

3. Results and Discussion

3.1. Changes in Precipitation

Results from the hypergeometric test (Figure 5) indicate a significant increase in the number of annual precipitation totals falling in the driest tercile of all totals post-1970s, while significantly fewer totals fell in the wettest tercile for the same period. Significance levels are approximately 0.05, but vary a little, because of the discrete nature of the hypergeometric distribution. The later portions of the rainy season seem to be primarily responsible for this reduction in annual totals; the procedure is repeated on monthly totals during the rainy season. February and April record significantly fewer years in their respective monthly lowest terciles, 1950–1970, while the months of January through April return significantly greater membership, 1981–2008, implying that the totals in the latter half of the rainy season have indeed diminished since the mid-1970s. This conclusion is reinforced by analysis of the memberships of the wettest tercile, where statistically significantly greater membership occurs in the same months prior to the proposed shift in climate and less afterwards. Additionally, these findings match and are expanded upon by other research wholly focused on examining climate variability in the same region of southern Africa [42].

Figure 5. Results from the hypergeometric test of the total annual precipitation amounts, based on their water (May–April) for the year from the periods 1950–1970 and 1980–2008.



3.2. Mean-Variance Analysis

Mean variance analysis as used here is based on a graphical analysis relying on diagrams to describe temporal change [27]. Mean-variance portraits are effective approaches for examining post-disturbance vegetation patterns [27]. NDVI mean-variance portraits for the entire landscape (Figure 6) indicate that prior to the proposed climate shift, the landscape as a whole was relatively well vegetated (as illustrated by high mean NDVI) and had fairly limited spatial heterogeneity (indicated by low NDVI variance). This observed landscape condition is likely the result of being measured during a period of more consistently high precipitation, and as such, vegetation amounts were higher throughout much of the landscape. NDVI in 1984 represents the landscape immediately following the climate shift (drying) and reveals a landscape with decreased amounts of vegetation, but increased heterogeneity, and reflects the impact of the precipitation reduction across this larger landscape, in the form of less vegetation and greater patchiness of cover. Vegetation appears to recover through the 1990s in terms of amount, with low spatial variance, but by 2009 has maintained the increased mean vegetation amount (but, it also has higher spatial variance). As such, it appears that both the amount of vegetation has recovered to a pre-disturbance regime, and also, the vegetation is more heterogeneous in 2009, potentially indicating a return to a more natural savanna state, *i.e.*, the inherent heterogeneity of savannas [2].

The temporal trajectory of mean-variance at the landscape scale is generally mirrored across the IGBP land cover classes, with the exception of the barren/barely vegetated land cover class (Figure 7). NDVI measures move across the plots from Quadrant 3 (high mean and low variance) prior to the shift, to the top left Quadrant 2 in 1984, returning eventually to similar mean NDVI values, but higher variance, in 2009. Since the majority (>70%) of the study area is classified as savanna, this is not unexpected. The land classes do differ in the extent to which mean NDVI decreases and NDVI variance changes.

The highest mean NDVI is observed within shrub and savanna (and some of the barely vegetated lands, which, based on field observation for a portion of the study area, are suspected to include many areas in which shrubs are present), and the lowest values are found in the grass and forest classes (and then the wetland and crops). Therefore, the increase in mean NDVI may represent an increase in shrub or savanna land cover and a decrease in forest and grasses. In terms of variance, the land cover classes with the highest NDVI variance values are forest and wetland, with savanna and bare representing lower NDVI variance values. The increased variance for forest and wetland may reflect an increased patchiness in these covers; whereas savanna and bare have a decreased variance, which would be reflective of a more homogeneous vegetation cover. As such, the savanna and bare classes may be ‘filling in’ and become more homogenous covers, whereas the forest and wetland classes are becoming patchier and more fragmented across the region. These mean-variance patterns for individual covers, once viewed as an entire landscape result, could reflect an increased savanna/shrub cover, with high mean NDVI values and, also, an increase in landscape heterogeneity, due to the different patterns of change across the different cover types, resulting in an overall increase in patchiness or heterogeneity at this landscape level.

The 1970 and 1990 results (Figure 7) show similar ranges and patterns of variance across land covers, although the mean values are higher for all classes in 1990. The higher mean values for the 1990 classes (*versus* 1970) could be due to the necessary difference in image acquisition dates. 1984 and 2009 present a greater range of variances, which may relate to the more extreme precipitation

events—1984 drought and 2009 large scale flooding. However, while the range and pattern across land covers are similar, the mean values for 1984 are the lowest of all years and all land covers as a result of the persistent drying of the climate after the mid-1970s. On the other hand, the very wet year of 2009 records mean values similar to the initial conditions of the 1970s, although all land covers, except for barely vegetated, return a slightly lower mean and considerably higher variances. Land covers appear to have rebounded from the climatic shift in the late 1970s, which shows a dramatic and consistent spatial trend of decreased NDVI across the entire landscape in 1984. By 1990, recovery appears to have set in across all land cover classes, resulting in high mean NDVI and low NDVI variance, with values being higher in terms of vegetation amount—but similar for variance across all classes. Finally, 2009 may represent a return of vegetation (mean and variance) similar to that of pre-disturbance, but NDVI variances are much larger in 2009—probably due in part to the higher precipitation and some flooding in that particular year—as well as potentially reflecting a return to a more ‘natural’ heterogeneous landscape for savanna ecosystems, where high heterogeneity reflects the multiple complex human and natural drivers of savanna systems [1,4].

If we look across land covers and less by temporal groupings alone (in essence, linking the dots for each land cover class sequentially by time in Figure 7), we can see that savanna and barely vegetated classes represent relatively flat patterns of change over time in terms of their trends and show quite limited dissimilarity in NDVI variance over time. The remaining classes all show the same patterns of the 1970s to 1984, with a decreased mean NDVI (as for savanna and barely vegetated), but a significant increase in NDVI variance. Likewise, the trend of increasing mean NDVI from 1984 to 1990 holds for all covers. However, for crops, forest, grasses, shrub and wetland, this trend is also accompanied by a significant decrease in NDVI variance, followed in 2009 by a decreasing NDVI mean (as for all land covers) and another significant increase in NDVI variance. When we view the land cover map (Figure 3), we see that the dominant land covers are savanna, followed by wetland and shrubs, and so, these are the major patterns of interest for this landscape.

The mean-variance patterns considered across the precipitation regimes (quintiles) are shown in Figure 8. Again, the trajectory of NDVI mean and variance is similar to that seen in the overall landscape, with decreasing mean NDVI values from 1970 to 1984, followed by a recovery period. Interestingly, the mean NDVI values by date are similar across the different precipitation zones; the real difference across zones lies instead in the variance. The first quintile represents the lowest mean annual rainfall region, increasing to the fifth quintile, which has the highest mean annual rainfall (Figure 3). Overlap exists between zone 1 and the wetland land cover class (Figure 2), with this driest annual precipitation region actually being composed of much of the Okavango Delta region. As such, much of the water input to this part of the landscape is related to runoff and water flow, separate from just the precipitation input experienced by the rest of the landscape. In general, this first quintile represents the highest NDVI variances, which occurs despite this region receiving low precipitation input and due to the presence of the wetland being fed by river flow and hydrological inputs. However, the pattern for NDVI variance differs, with the middle quintiles (second, third and fourth) showing very little initial change in NDVI variance. The driest part of the study area (first quintile) has the highest NDVI variance across each of the first three time steps; however, in 2009, the NDVI variance of the wettest part of the study area exceeds that of the driest. This level of analysis (related to rainfall zones) provides an assessment that begins to address the role of localized water availability (regardless

of source) in the patterns of vegetation change as compared to the landscape scale analysis, which considers a broader view of heterogeneity. The observed patterns in the rainfall zone mean-variance analysis may well link to the extreme year of 2009, where flooding covered much of the region, and may well be reflected in this pattern of higher NDVI variance.

Considering the overall landscape mean-variance trends in terms of NDVI mean values, the trend is consistent over time, with the decrease in mean NDVI post-1970s resulting from the shift in climate being felt across the entire landscape (Figure 6), across all land cover types (Figure 7) and across all precipitation zones (Figure 8), thus truly showing the significant impact this change of regime had across the region. This was followed by a decade of recovery and adaptation to the new precipitation regime—savannas are adaptable environments and, indeed, are known by their heterogeneity over space and time. Thus, by 1990, we see the highest mean NDVI values and still relatively low variance. By 2009, the landscape appears to have stabilized once more, with mean NDVI values being similar to the initial state of the landscape in the 1970s, and the main differences are due to the higher NDVI variance values, which may well reflect a slightly different vegetated state than was previously present in this region. The occurrence of extreme events, such as in 2009, when flooding occurred throughout much of the southern portion of the study area (Okavango Delta area and Caprivi Strip, Namibia), is also reflected in the variance of NDVI values for 2009 (Figures 6–8). Overall, though, we can see that a higher mean NDVI and a higher variance of NDVI potentially represents a resilient landscape returning to its inherent heterogeneity of cover, as expected for savanna ecosystems [1,2,4].

Figure 6. Results from mean variance analysis for the entire landscape, with each dot representing one image date, as indicated.

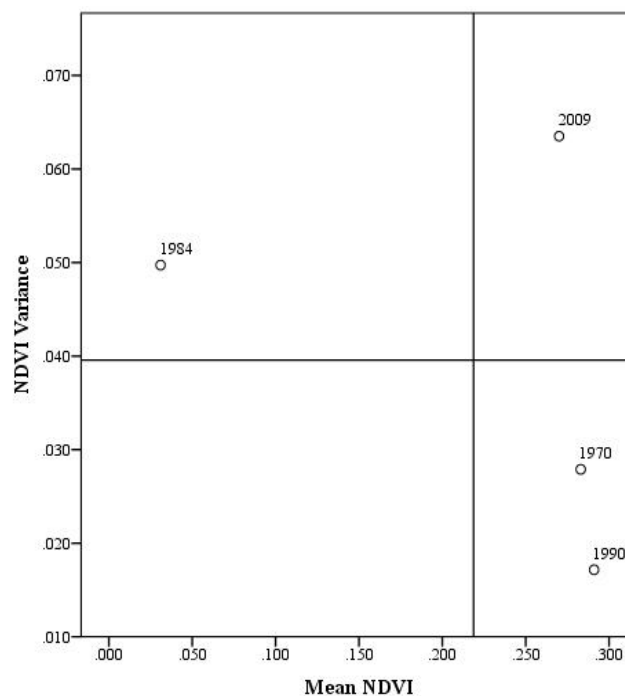


Figure 7. Results for mean variance analysis for each land cover class (barren/barely vegetated, croplands, wetlands, grasslands, savannas, shrub lands, forest) from the IGBP land cover classes.

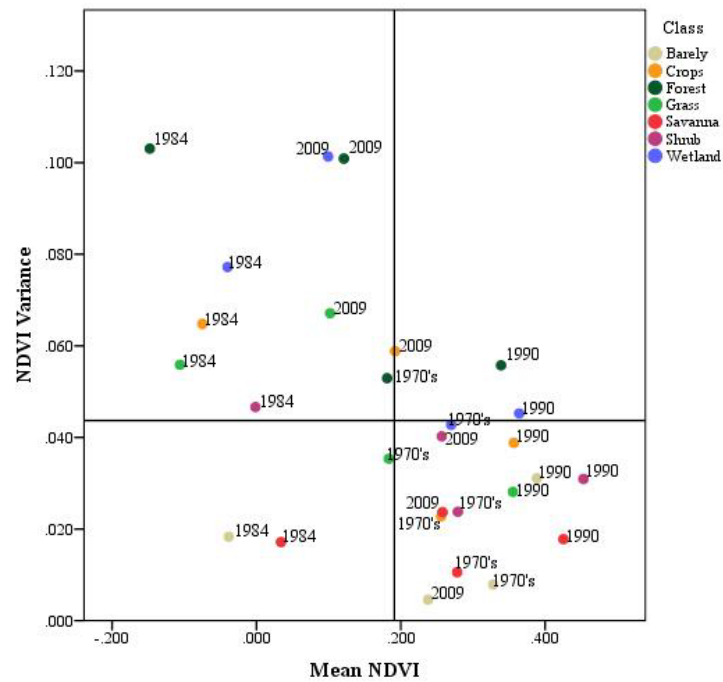
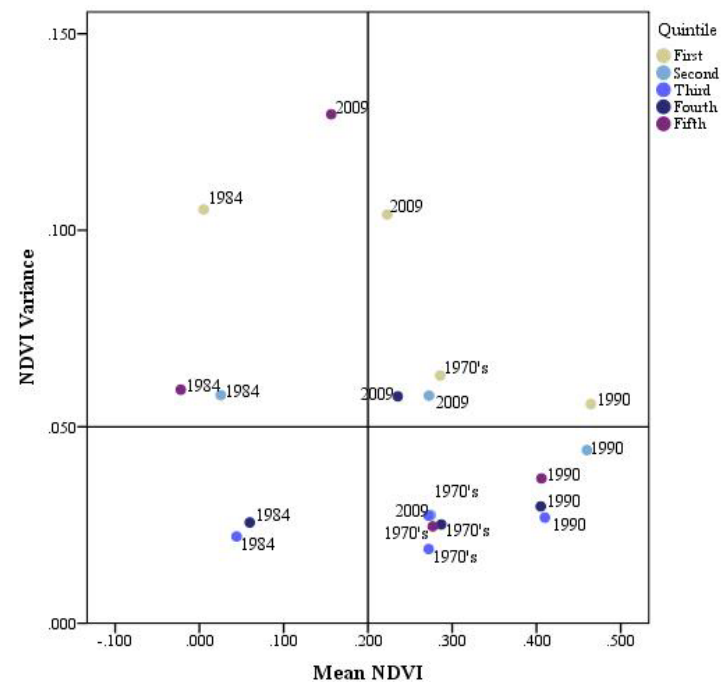


Figure 8. Results for mean variance analysis for each precipitation class (quintiles), with the first quintile representing the driest to the fifth representing the wettest areas on the landscape.



3.3. Persistence Analysis

The trends and imagery discussed so far represents a predominantly aspatial analysis, yet there are also many interesting and fine scale patterns occurring over space. In order to address the spatial

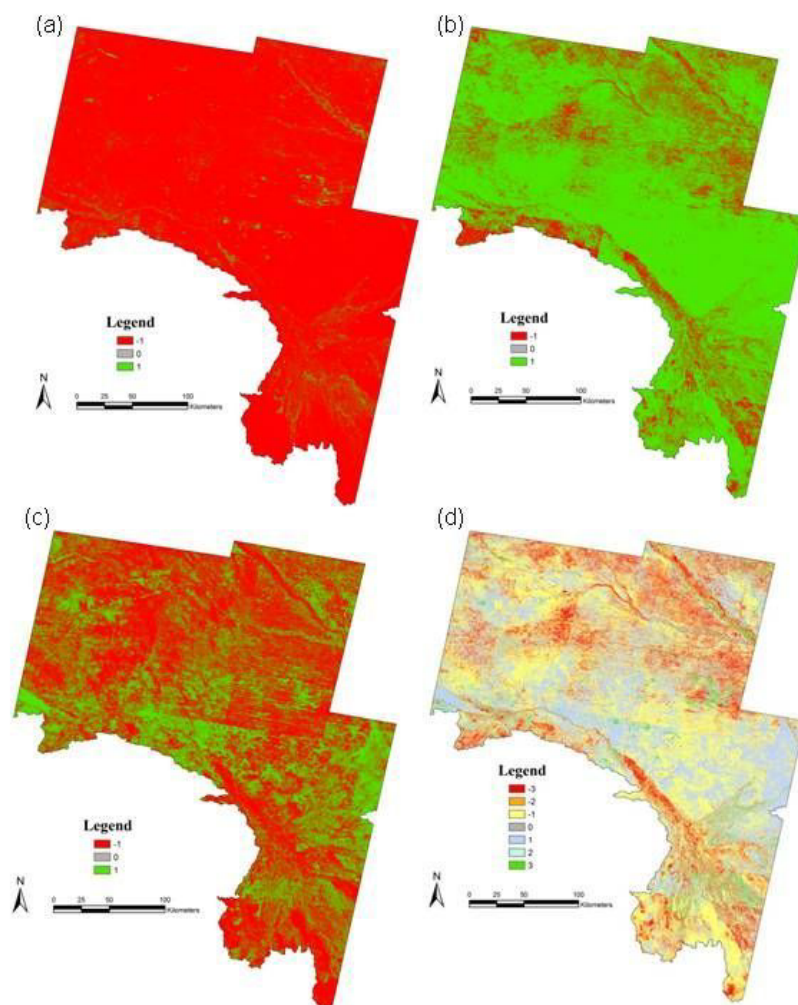
patterns across time, we undertook a persistence trend analysis conceptually similar to that of Lanfredi *et al.* [54], which reveals the degree of consistency of temporal trends over time. Given that the driver of change across the landscape has been a significant shift in climate and subsequent recovery period, we would not necessarily expect to see consistent trends over time, yet it is interesting to consider each of the time step intervals of analysis and examine whether the spatial patterns generally match those observed by time, land cover class and precipitation zone. Such a comparison also permits the detection of portions of the landscape, which consistently differ from the overall temporal trends. Patterns of spatial persistence of NDVI values for each date are compared to the initial conditions of 1970 (Figure 9). From the 1970s to 1984, we see the expected decrease in NDVI over the entire study region (Figure 9(a)). Likewise, 1970 to 1990 illustrates the rebound and recovery in full effect with increased NDVI values, as we saw in Figures 5–7. However, not all regions follow this dominant trend, specifically, the wetland regions and the highest and lowest precipitation zones, which evince more negative trends in NDVI change. By 2009, the landscape seems to be returning to its initial state (according to Figures 6–8), as reflected by almost equal areas of increase and decrease in NDVI (Figure 9(c)), but, overall, declining slightly. Given that the persistence threshold here is set at 0.01 in order to filter out small fluctuations and only highlight major changes, then the trends shown in Figure 9 can be seen to support the existing contentions, while furnishing interesting spatial information about which areas or cover types seem to behave contrary to the dominant pattern. Figure 9(d) summarizes these persistence trends by summing the individual coverages at a pixel level to reveal the overall trend of a slight decrease in NDVI. Areas of consistently declining NDVI are the wetland regions and precipitation zones 1 and 5 (highest and lowest quintiles). Smaller areas of consistent trends are found in the Savanna land cover class. Thus the spatial trends add an interesting component to the analysis, particularly when linked to the land cover and precipitation information. The use of the mean-variance analysis in tandem with the spatial persistence integrates continuous indices for assessment of land cover change within a framework, which considers landscape trajectories post-climate shock and is undertaken at a scale that is fine enough to link to surface processes. While MODIS (250 m–1 km and only since late 1999) or AVHRR (1.1–8 km, 1981–2006) could provide more time points for study, they do not provide the continuity of the Landsat mission, the pre-climatic impact event timing (earliest for AVHRR is July 1981) or the fine spatial scale we felt essential for this analysis and for increasing our understanding of this highly dynamic savanna region.

3.4. Methodological Mean-Variance Framework for Resilience Context

The concepts of resilience and the indicators and metrics mentioned in Table 1 can be related to the landscape under study. Inevitably, the dates selected for the study influence the findings to some degree, yet selection of the largest range of available dates and data, compilation of the imagery and the number of time periods studied represents a significant data source and contribute to the limited studies of change within this landscape. Linkages between precipitation and vegetation addressed in previous studies are here viewed from a longer term perspective within a resilience framework and considered explicitly the climatic shift of the late 1970s as a significant environmental perturbation, with subsequent periods representing the response and potential recovery of this dry land ecosystem to this

‘shock’. We therefore examine the landscape more as a whole and attempt to address the longer term survival or likelihood of adaptation of this system, as future climatic shocks are predicted to occur.

Figure 9. Results from the NDVI persistence analysis for each of the time steps: (a) 1970–1984, (b) 1984–1990 and (c) 1990–2009; (d) cumulative change in NDVI across the entire time period. These results indicate an initial decrease in NDVI from 1970 to 1984 for the majority of the landscape, followed by increases in NDVI values for much of the study area from 1984 to 1990, followed by mixed changes within the landscape from 1990 to 2009.



The amplitude of the change in vegetation resulting from the perturbation of the climate system existed throughout the entire landscape (in terms of space), present across all land covers and numerically expressed as a drop in the mean NDVI of between 0.3 and 0.4, although the slightly later image date for the 1984 image may contribute to this. This constitutes a significant and widespread response, as is clearly seen in Figure 9. The malleability of the landscape between the 1970s and 2009 is difficult to assess based on NDVI alone, but examination of the range of values of mean and variance of the variable across land covers suggests a potential shift in vegetation state. Increases in mean NDVI during the 1990s appear to support this, although the return to values similar to the 1970s by 2009 may reflect the increased precipitation and extensive flooding during the last few years of the

study. A shift in cover types, therefore, cannot be completely ascertained, although one seems likely, given the changes noted across the region. System dampening and oscillations are more difficult to establish, given the temporal resolution of the data limiting frequency of observations post-disturbance. However, at the temporal scale of the data, Figures 6–8 begin to illustrate the post-disturbance temporal dynamics. A finer temporal analysis would provide a more substantive analysis of this particular measure of system resilience. Finally, we attempt to address the system's hysteresis by examining the apparently different paths of degradation and post-climate-shift collapse, compared to that of restoration and recovery, as evidenced by the shape of the pathways over time, across land cover type and across precipitation zones. The results are substantive, as when addressed across various types of gradients or classifications, the results still hold true. The addition of the spatial persistence trends adds weight to the discussion, depicting some clear spatial patterns of NDVI decline and increase, but, overall, a landscape in which over 70% of the region is close to its initial position from 35 years earlier (NDVI values in persistence coverages on Figure 9(d) of -1 , 0 or $+1$), seemingly showing an adaptable landscape, even in the face of a significant and long-term climatic shift.

The approach used here provides information regarding landscape status as it relates to climate, with specific reference to landscape changes post-climate shift, as compared to the pre-shift status of the landscape. In doing so, preliminary linkages between the dominant driver of landscape change for this region—precipitation—and land cover are established. Such integration of continuous characterizations of land cover is needed within heterogeneous landscapes, as it provides a more representative analysis of land cover change within savanna ecosystems. While the limitations of this are similar to those associated with most remote sensing-based analyses, namely, that the data available corresponds to a set number of dates and offers no knowledge of the status of the landscape during the intervening time periods, the linkages to precipitation patterns over the longer time-frame and current understanding of precipitation as the main driver in this system allow us to make some significant conclusions regarding change.

The assessment of the landscape in its entirety, as well as pixel by pixel is also less commonly used within land cover change analyses and supports a landscape-level study. Conceptualization of the landscape as a whole is central to integrating resilience concepts in a quantifiable manner and progresses the study of landscape-level change by increasing the incorporation of landscape complexity within measurements of land cover change. While this is important to most ecosystems, this work specifically extends upon Washington-Allen *et al.* [27] by examining the applicability of such an approach for savanna ecosystems, which cover expansive areas and which, from a socio-ecological perspective, are considered to be highly vulnerable to future climatic shocks.

4. Conclusions

It is difficult to observe a clear unambiguous climatic shock to any system and then to have a period of stability to observe the recovery of the system. However, the second half of the 1970s provides a fairly universally accepted shift in the operation of global circulation [16,18,42], and its local impacts are quite clear and persistent throughout the time period under consideration here [19], although there is some question as to whether the data from 2009 may actually represent a shift back to wetter conditions [55], and only an extended time period into the future will determine this. Nonetheless, the

last two decades of the twentieth century offer an ideal period to investigate the impacts of both a decline in annual precipitation and a greater variability associated with ENSO on vegetation in an ecosystem that is thought to be extremely sensitive to such fluctuations.

In terms of landscape resilience, we argue that the system has responded to the ‘shock’ or ‘perturbation’ caused by the shift in climate during the 1970s and has adapted and responded in such a way that the mean vegetation has returned to a similar state as the ‘initial’ point, though with greater spatial heterogeneity than was previously evident. These vegetation responses to precipitation changes suggest that the vegetation in the region (most of which is native) is capable of retaining key system characteristics (as measured by NDVI) despite changes in climate, though this does not necessarily mean that it will stay this way under future predicted climate changes, and it does not exclude the idea that some of the recovery also represents a shift to increased shrub growth (bush encroachment is considered a significant degradation to this system). Other arguments could be applied to explain the observed patterns, such as the natural growth cycle of savanna vegetation, which is postulated to occur on a predominantly 30-year cycle [56]. This could also explain the landscape mean decrease and rebound of NDVI post-1970s, with a natural death and regeneration of the landscape, although it is unlikely that such a phenomenon would occur simultaneously over such a large landscape and, so, consistently across the land cover types (Figure 7). The time-dependence of this analysis is a limitation that will be addressed in future research. Specifically, it is assumed here that the temporal resolution and extent adequately captures the response of vegetation to the change in climate; this limitation of the study is inherent in the dataset used (imagery), though the trade-off of use of this dataset as the predominant source of information is that it supports the quantification of change at the landscape-scale with systematically recorded observations pre- and post-climate shift. Future analyses will decompose this temporal trend further, utilizing monthly data throughout the entire period of study. This will require an increase in spatial scale (AVHRR and MODIS), and so, the fine grained spatial resolution and detail from this study will be sacrificed for improved temporal resolution. Such trade-offs are themselves worthy of future study. Additionally, this research can be used to ascertain types of land cover shifts, as these images provide a basis for more in-depth examination of land cover change, and sub-pixel linear unmixing to determine components of vegetation at this finer spatial scale will also be undertaken. Clearly, there are some major shifts even within this system, which appears to eventually adapt to drier conditions. The land cover data used here (Figure 2) is static, and so, changes in cover type were not evaluated, only changes in NDVI. However, this research experiments with the use of continuous measures of land cover, such as NDVI, within a resilience framework, which couples climatological shifts with biophysical patterns in order to better characterize the long-term changes within the ecosystem. Future research will link these changes much more explicitly to climate at monthly or annual time steps and to finer land cover classifications.

Acknowledgments

This study was funded by the NASA LCLUC Project #NNX09AI25G, titled “The Role of Socioeconomic Institutions in Mitigating Impacts of Climate Variability and Climate Change in Southern Africa” PI: Jane Southworth.

Conflict of Interest

The authors declare no conflict of interest.

References

1. Hill, M.J.; Hanan, N.P. Savannas: Biogeographical and Ecological Perspectives. In *Ecosystem Function in Savannas: Measuring and Modeling at Landscape to Global Scales*; CRC Press: Boca Raton, FL, USA, 2010; pp. 1–10.
2. Scholes, R.J.; Archer, S.R. Tree-grass interactions in savanna. *Ann. Rev. Ecol. Systemat.* **1997**, *28*, 517–544.
3. Peters, D.P.C.; Havstad, K.M. Nonlinear dynamics in arid and semi-arid systems: Interactions among drivers and processes across scales. *J. Arid Environ.* **2006**, *65*, 196–206.
4. Scholes, R.J.; Walker, B.H. *An African Savanna: Synthesis of the Nylsvley Study*; Cambridge University Press: Cambridge, UK, 1993; pp. 264–267.
5. Reynolds, J.F.; Smith, D.M.S.; Lambin, E.F.; Turner, B.L., II; Mortimore, M.; Batterbury, S.P.; Downing, T.E.; Dowlatabadi, H.; Fernandez, R.J.; Herrick, J.E.; *et al.* Global desertification: building a science for dryland development. *Science* **2007**, *316*, 847–851.
6. Hüttich, C.; Herold, M.; Wegmann, M.; Cord, A.; Strohbach, B.; Schmullius, C.; Dech, S. Assessing effects of temporal compositing and varying observation periods for large-area land-cover mapping in semi-arid ecosystems: Implications for global monitoring. *Remote Sens. Environ.* **2011**, *115*, 2445–2459.
7. Herold, M.; Mayaux, P.; Woodcock, C.E.; Baccini, A.; Schmullius, C. Some challenges in global land cover mapping: An assessment of agreement and accuracy in existing 1 km datasets. *Remote Sens. Environ.* **2008**, *112*, 2538–2556.
8. Jung, M.; Henkel, K.; Herold, M.; Churkina G. Exploiting synergies of global land cover products for carbon cycle modeling. *Remote Sens. Environ.* **2006**, *101*, 534–553.
9. Lambin E.F.; Geist, H.J. *Land Use and Land Cover Change: Local Processes and Global Impacts*; Springer: New York, NY, USA, 2005.
10. Foody, G.M. Monitoring the magnitude of land-cover change around the southern limits of the Sahara. *Photogramm. Eng. Remote Sensing* **2001**, *67*, 841–847.
11. Chamaille-Jammes, S.; Fritza, H.; Murindagomo, F. Spatial patterns of the NDVI-rainfall relationship at the seasonal and interannual time scales in an African savanna. *Int. J. Remote Sens.* **2006**, *27*, 5185–5200.
12. Vanacker, V.; Linderman, M.; Lupo, F.; Flasse, S.; Lambin, E. Impact of short term rainfall fluctuation on interannual land cover change in sub-Saharan Africa. *Global Ecol. Biogeogr.* **2005**, *14*, 123–135.
13. Richard, Y.; Pocard, I. A statistical study of NDVI sensitivity to seasonal and interannual rainfall variations in Southern Africa. *Int. J. Remote Sens.* **1998**, *19*, 2907–2920.
14. Fuller, D.O.; Prince, S.D. Rainfall and foliar dynamics in tropical southern Africa: Potential impacts of global climatic change on savanna vegetation. *Clim. Change* **1996**, *33*, 69–96.

15. Townshend, J.R.G.; Justice, C.O. Analysis of the dynamics of African vegetation using the normalized difference vegetation index. *Int. J. Remote Sens.* **1986**, *7*, 1435–1445.
16. Chavez, F.; Ryan, J.; Lluich-Cota, S.; Niquen, M. From anchovies to sardines and back: Multidecadal change in the Pacific ocean. *Science* **2003**, *299*, 217–221.
17. Nicholson, S.E. The nature of rainfall variability over Africa on time scales of decades to millenia. *Glob. Planet. Change* **2000**, *26*, 137–158.
18. Hare, S.R.; Mantua, N.J. Empirical evidence for North Pacific regime shifts 1977 and 1989. *Prog. Oceanogr.* **2000**, *47*, 103–145.
19. Batisani, N.; Yarnal, B. Rainfall variability and trends in semi-arid Botswana: Implications for climate change adaptation policy. *Appl. Geogr.* **2010**, *30*, 483–486.
20. Nicholson, S.E.; Leposo, D.; Grist, J. The relationship between El Niño and drought over Botswana. *J. Clim.* **2001**, *14*, 323–335.
21. Reason, C.J.C.; Mulenga, H.M. Relationships between South African rainfall and SST anomalies in the southwest Indian Ocean. *Int. J. Climatol.* **1999**, *19*, 1651–1673.
22. Shi, G.; Ribbe, J.; Cai, W.; Cowan, T. Multidecadal variability in the transmission of ENSO signals to the Indian Ocean. *Geophys. Res. Lett.* **2007**, *34*, L10610.
23. Mason, S. El Niño, climate change, and Southern African climate. *Environmetrics* **2001**, *12*, 327–345.
24. Chown, S. Temporal biodiversity change in transformed landscapes: A southern African perspective. *Phil. Trans. R. Soc.* **2010**, *365*, 3729–3742.
25. Magadza, C. Climate change: some likely multiple impacts in Southern Africa. *Food Policy* **1994**, *19*, 165–191.
26. Washington-Allen, R.A.; Ramsey, R.; West, N.E. Spatiotemporal mapping of the dry season vegetation response of sagebrush steppe. *Comm. Ecol.* **2004**, *5*, 69–79.
27. Washington-Allen, R.A.; Ramsey, R.; West, N.E.; Norton, B.E. Quantification of the ecological resilience of drylands using digital remote sensing. *Ecol. Soc.* **2008**, *13*, 33.
28. Goheen, J.; Young, T.; Keesing, F.; Palmer, T. Consequences of herbivory by native ungulates for the reproduction of a savanna tree. *J. Ecol.* **2007**, *95*, 129–138.
29. Ringrose, S.; Matheson, W.; Tempest, F.; Boyle, T. The development and causes of range degradation features in southeast Botswana using multi-temporal Landsat MSS imagery. *Photogramm. Eng. Remote Sensing* **1990**, *56*, 1252–1262.
30. Adger, W.N.; Hughes, T.P.; Folke, C.; Carpenter, S.; Rockstrom, J. Social-ecological resilience to coastal disasters. *Science* **2005**, *309*, 1036–1039.
31. Carpenter, S.R.; Walker, B.H.; Anderies, J.M.; Abel, N. From metaphor to measurement: Resilience of what to what? *Ecosystems* **2001**, *4*, 765–781.
32. Westman, W.E.; O’Leary, J. Measures of resilience: the response of coastal sage scrub to fire. *Vegetatio* **1986**, *65*, 179–189.
33. Simoniello, T.; Lanfredi, M.; Liberti, M.; Coppola, R.; Macchiato, M. Estimation of vegetation cover resilience from satellite timer series. *Hydrol. Earth Syst. Sci. Discuss.* **2008**, *5*, 511–546.
34. Dougill, A.; Trodd, N. Monitoring and Modelling Open Savannas Using Multisource Information: Analyses of Kalahari Studies. *Global Ecol. Biogeogr.* **1999**, *8*, 211–221.
35. Frost, P.G.H.; Robertson, F. Fire: The Ecological Effects of Fire in Savannas. In *Determinants of Tropical Savannas*; Walker, T.S., Walker, B.H., Eds.; IRL Press: Oxford, UK, 1987; pp. 93–140.

36. Walker, B.H.; Noy-Meir, I. Aspects of the Stability and Resilience of Savanna Ecosystems. In *Ecology of Tropical Savannas*; Huntley, B.J., Walker, B.H., Eds.; Springer Verlag: Berlin, Germany/New York, NY, USA, 1982; pp. 577–590.
37. Martiny, N.; Camberlin, P.; Richard, Y.; Philippon, N. Compared regimes of NDVI and rainfall in semi-arid regions of Africa. *Int. J. Remote Sens.* **2006**, *27*, 5201–5223.
38. Farrar, T.J.; Nicholson, S.E.; Lare, A.R. The influence of soil type on the relationships between NDVI, rainfall, and soil moisture in semiarid Botswana. II. NDVI response to soil moisture. *Remote Sens. Environ.* **1994**, *50*, 121–133.
39. Scanlon, T.M.; Caylor, K.K.; Manfreda, S.; Levin, S.A.; Rodriguez-Iturbe, I. Dynamic response of grass cover to rainfall variability: implications for the function and persistence of savanna ecosystems. *Adv. Water Resour.* **2005**, *28*, 291–302.
40. Stige, L.; Stave, J.; Chan, K.; Ciannelli, L.; Pettorelli, N.; Glantz, M.; Herren, H. The effect of climate variation on agro-pastoral production in Africa. *Proc. Natl. Acad. Sci. USA* **2006**, *103*, 3049–3053.
41. Area, Kavango-Zambezi Transfrontier Conservation. *Mitigation of Human-Elephant Conflict in the Kavango-Zambezi Transfrontier Conservation Area through Community Based Problem Animal Control, with Particular Reference to the Use of Chilli Peppers*; 2006. Available online: <http://www.dlist-benguela.org/sites/default/files/doclib/human%20elephant%20conflict%20TFCA.pdf> (Accessed on 3 August 2013).
42. Gaughan, A.E.; Waylen, P.R. Spatial and temporal precipitation variability in the Okavango-Kwando-Zambezi catchment, southern Africa. *J. Arid Environ.* **2012**, *82*, 19–30.
43. Archibald S.; Scholes R.J. Leaf green-up in a semi-arid African savanna—Separating tree and grass responses to environmental cues. *J. Veg. Sci.* **2007**, *181*, 583–594.
44. Jensen, J.R. *Introductory Digital Image Processing: A Remote Sensing Perspective*, 3rd ed.; Prentice-Hall: New York, NY, USA, 2005.
45. Green, G.M.; Schweik, C.M.; Randolph, J.C. Retrieving Land-Cover Change Information from Landsat Satellite Images by Minimizing Other Sources of Reflectance Variability. In *Seeing the Forest and the Trees: Human–Environment Interactions in Forest Ecosystems*; Moran, E.F., Ostrom, E., Eds.; MIT Press: Cambridge, MA, USA, 2005.
46. Markham, B.L.; Barker, J.L. Landsat MSS and TM post-calibration dynamic rangers, exoatmospheric reflectance and at-satellite temperatures. *EOSAT Landsat Tech. Notes* **1986**, *1*, 3–8.
47. Guerschman, J.P.; Hill, M.J.; Renzullo, L.J.; Barrett, D.J.; Marks, A.S.; Botha, E.J. Estimating fractional cover of photosynthetic vegetation, non-photosynthetic vegetation and bare soil in the Australian tropical savanna region upscaling the EO-1 Hyperion and MODIS sensors. *Remote Sens. Environ.* **2009**, *113*, 928–945.
48. Schmidt, H.; Karnieli, A. Remote Sensing of the seasonal variability of vegetation in a semi-arid environment. *J. Arid Environ.* **2000**, *45*, 43–59.
49. Running, S.W.; Loveland, T.L.; Pierce, L. A vegetation classification logic based on remote sensing for use in global biogeochemical models. *Ambio* **1994**, *23*, 77–81.
50. Sedano, F.; Gong, P.; Ferrao, M. Land cover assessment with MODIS imagery in southern African Miombo ecosystems. *Remote Sens. Environ.* **2005**, *98*, 429–441.

51. Adler, R.F.; Huffman, G.J.; Change, A.; Ferraro, R.; Xie, P.-P.; Janowiak, J.; Rudolf, B.; Schneider, U.; Curtis, S.; Bolvin, D.; *et al.* The version-2 Global Precipitation Climatology Project (GPCP) monthly precipitation analysis (1979–present). *J. Hydrometeorol.* **2003**, *4*, 1147–1167.
52. Curtis, S.; Adler, R.F. ENSO indices based on patterns of satellite-derived precipitation. *J. Clim.* **2000**, *13*, 2786–2793.
53. Pickup, G.; Foran, B.D. The use of spectral and spatial variability to monitor cover change on inert landscapes. *Remote Sens. Environ.* **1987**, *23*, 361–363.
54. Lanfredi, M.; Simoniello, T.; Macchiato, M. Temporal persistence in vegetation cover changes observed from satellite: Development of an estimation procedure in the test site of the Mediterranean Italy. *Remote Sens. Environ.* **2004**, *93*, 565–576.
55. Swanson, K.L.; Tsonis, A.A. Has the climate recently shifted? *Geophys. Res. Lett.* **2009**, *36*, L06711.
56. Meyer, K.; Wiegand, K.; Wards, D.; Moustakas, A. The rhythm of savanna patch dynamics. *J. Ecol.* **2007**, *95*, 1306–1315.

© 2013 by the authors; licensee MDPI, Basel, Switzerland. This article is an open access article distributed under the terms and conditions of the Creative Commons Attribution license (<http://creativecommons.org/licenses/by/3.0/>).